JOURNAL OF MATERIALS SCIENCE 27 (1992) 3835–3842

Microstructural analysis of isothermally exposed Ti/SiC metal matrix composites

I. W. HALL, J.-L. LIRN
Materials Science Program, University of Delaware, Newark, DE 19716, USA
Y. LEPETITCORPS, K. BILBA
Laboratoire de Chimie du Solide du CNRS, Université de Bordeaux I, 33405 Talence cedex, France

Specimens of diffusion-bonded titanium metal matrix composites have been subjected to thermal exposure treatments and examined principally by transmission electron microscopy. The fibres investigated were SCS-6™ and Sigma™. The fibre/matrix reaction layers have been shown to consist of titanium carbide and two titanium silicides. The reaction proceeds by the initial formation of a layer of TiC followed by a layer of mixed silicides, Ti_5Si_4 and Ti_5Si_3. Extensive porosity is generated during the reaction and this prevents the formation of a completely protective interfacial layer.

1. Introduction

Titanium matrix composites have been under development for several years and are candidate materials for aircraft structural applications, particularly those at moderately elevated temperatures where strength/weight ratio is of paramount importance. Although many experimental manufacturing methods are currently under investigation, the majority of these composites to date have been made via a diffusion-bonding technique and this is projected to continue with advances in titanium alloy and aluminide foil production. A major drawback to many production routes, including diffusion bonding, is that the composite is subjected to heat and pressure for a considerable length of time and adverse chemical reactions occur at the fibre/matrix interface.

Efforts have been made to mitigate the seriousness of these reactions by compositionally tailoring the surface of the fibre to reduce its reactivity with the matrix and the SCS-6™ and Sigma™ fibres used in the present work represent the results of such development programmes. Another approach is to coat the fibre surface with a protective layer designed to separate fibre and matrix and hence prevent attack [1]. Potential coatings include oxides, carbides and silicides and part of the present investigation concerned the suitability of titanium disilicide as a candidate for coating.

The key to further fibre development or to the application of the present generation of fibres is to understand the reactions at the interface. Much work has already been performed in the Ti/SiC system using powder metallurgy techniques and earlier-generation reinforcing fibres as well as some in the SCS-6/Ti–6Al–4V system which is the principal focus of current attention [2–5]. However, studies of this system are far from conclusive and this research was initiated to develop a better understanding of the role of isothermal exposure in exacerbating the adverse fibre/matrix reactions and to identify the reaction products and mechanisms. A model is proposed for the observed reaction mechanism.

2. Experimental procedure

Two different composites were used, the first being the commercially available SCS-6/Ti–6Al–4V composite. The composite was in the form of rectangular sheet, ~ 1.5 mm thick, consisting of 8 plies of 145 μm SiC fibres. The structure of these fibres and their compositionally graded protective coating have been described elsewhere [6]. The second system contained a layer of titanium disilicide between the fibre and matrix because previous work had shown that silicides were produced during fabrication and isothermal exposure. The 1 μm layer of $TiSi_2$ was deposited by chemical vapour deposition (CVD) on to Sigma fibres, and diffusion bonded into a commercially pure titanium matrix. Sigma fibres differ from SCS-6 in being only 100 μm diameter and having a surface coating enriched in silicon instead of carbon. Also they are deposited on a tungsten precursor rather than carbon and the precursor/fibre reactions may be of importance for long-term thermal stability. Investigation of these samples was intended to indicate whether titanium silicide had potential as a protective coating. The second composite is denoted $Ti/TiSi_2/SiC$.

All heat treatments were carried out on composites encapsulated in evacuated silica tubes so as to avoid oxygen pick-up. Polished and lightly etched samples were examined by optical and scanning electron microscopy (SEM). The thickness of the SCS-6/Ti–6Al–4V reaction layer was monitored as a function of exposure temperature and time, in order to investig-

0022–2461 © *1992 Chapman & Hall*

ate the reaction kinetics. The thickness of the reaction zone (RZ) was determined at > 40 locations for each sample. Thin foils for transmission electron microscopy (TEM) and electron energy loss spectroscopy (EELS) were prepared from transverse sections by low-speed diamond wheel sectioning and standard ion milling methods; they were examined in a Jeol 2000FX or Philips EM400T.

3. Results

The thickness of the RZ in as-fabricated composite appeared to be about 1 μm and increased significantly with isothermal exposure as shown in Fig. 1. For clarity, standard deviation data are shown for the 1050 °C data only. For times up to 24 h, the reaction follows the normal parabolic law at 950 °C with a single rate constant of 1.85×10^{-2} μm $s^{-1/2}$. However, at higher temperatures two rate constants are found, corresponding to short and long times. The rate constants at 1000 °C were 6.41×10^{-2} and 2.97×10^{-2} μm $s^{-1/2}$ at $t < 10$ h and $t > 10$ h, respectively. The discontinuities in the reaction rate data correspond closely to the times at which complete consumption of the protective coating of the fibre was observed to have occurred and the underlying SiC itself was exposed. Based on the parabolic rate

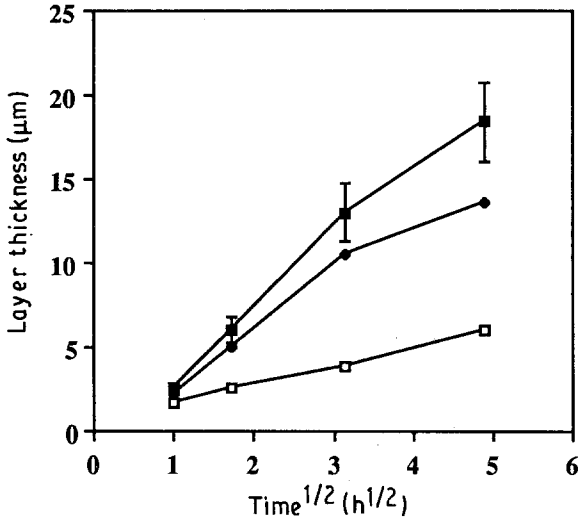

Figure 1 Reaction layer thickness as a function of square root of isothermal exposure time for SCS-6/Ti–6Al–4V at (□) 950 °C, (◆) 1000 °C, and (■) 1050 °C.

equation

$$y^2 = kt \quad (1)$$

and the usual Arrhenius equation the activation energy for the process is calculated from the equation

$$k = k_0 \exp\left(-\frac{Q}{2RT}\right) \quad (2)$$

This yields apparent activation energies of 95 630 cal mol^{-1} for the process occurring at short times and 74 060 cal mol^{-1} for that occurring at longer exposure times.

The detailed structure of the RZ in the as-fabricated composite could not be resolved in the SEM but increasing exposure times and/or higher temperatures produced a complex RZ containing distinct layers. Finally after 24 h at 1050 °C, a concentric ring structure developed around the fibre, Fig. 2a. Extensive

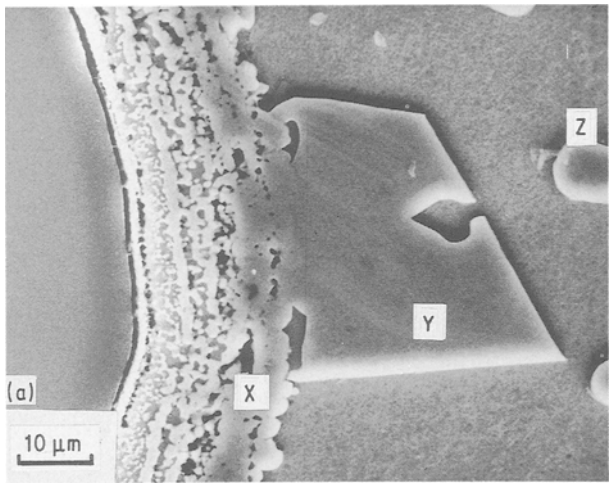

Figure 2 (a) Scanning electron micrograph showing the RZ of SCS-6/Ti–6Al–4V after 24 h at 1050 °C. Region "X" of RZ is formed by reaction of the matrix with fibre surface coating. (b) EDS spectrum of crystal "Y": analysis indicates Ti_3AlC. (c) EDS spectrum of crystal "Z": analysis indicates TiC.

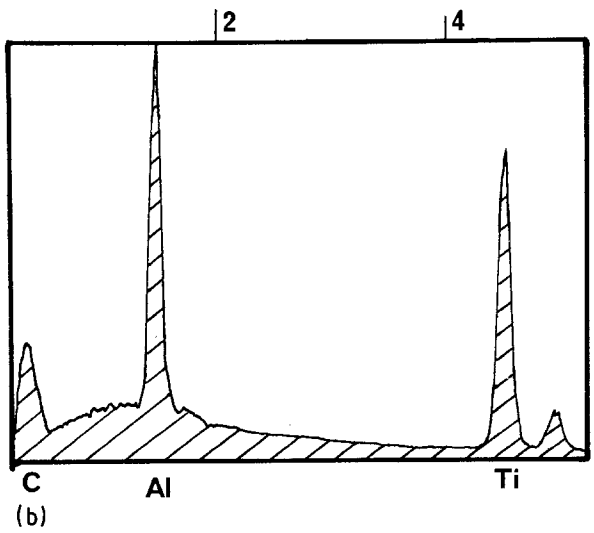

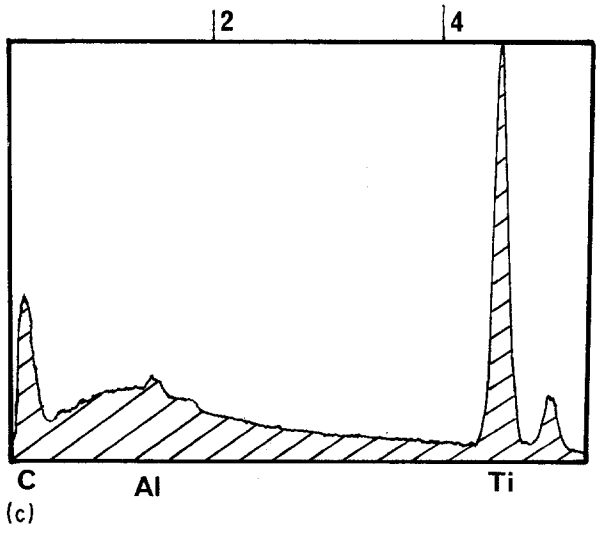

porosity was clearly seen but it also was approximately confined to concentric bands. It has been shown elsewhere [7, 8] that the outer layer, labelled "X" in Fig. 2a arises from the consumption of the protective layer, and the inner layers arise from the consumption of the SiC itself. Energy dispersive X-ray spectroscopy (EDS) showed that the outer layer apparently contained an intimate mixture of titanium silicide and titanium carbide while the rings were alternating layers of these phases. No oxygen pick-up was detected in the RZ.

At these thermal exposure times and/or temperatures, large angular crystals formed both within the matrix and at the RZ/matrix interface. EDS spectra of the large angular grain labelled "Y" at the interface in Fig. 2a showed it to contain titanium, aluminium and carbon, Fig. 2b. Standardless analysis of the titanium and aluminium peaks yielded an atomic composition close to Ti_3Al and the particle is, therefore, believed to be Ti_3AlC. Similar angular grains lying entirely within the matrix (labelled "Z") contained only titanium and carbon, and are, therefore, identified as TiC.

The effects of isothermal exposure on $Ti/TiSi_2/SiC$ specimens were closely analogous in that concentric shells of reaction product eventually built up at long exposure times.

TEM and further EDS analyses were then used to examine these structures in greater detail. In the as-fabricated SCS-6/Ti–6Al–4V composite, the average thickness of the RZ was found to be ~ 0.6 μm, Fig. 3a. This figure shows the matrix at lower right and the two outer layers of the SCS coating at upper left. Close examination of the RZ showed that it consisted of three distinct layers. In contact with the outer surface of the fibre was a crystalline layer ~ 100 nm thick, in which the grain size was of the order of 25 nm. Electron diffraction ring patterns obtained from this layer confirmed that it consisted uniquely of crystallites of TiC, Fig. 3b. The second layer consisted of substantially coarser grains growing outwards towards the matrix and these grains were ~ 300 nm in size. They were readily identified by electron diffraction as TiC, and a typical convergent beam pattern is inset in Fig. 3a showing the four-fold symmetry of the cubic TiC structure of the crystal indicated.

The third layer, adjacent to the matrix, consisted of elongated grains about 200 nm thick and with an aspect ratio of ~ 3. They lay parallel to the interfacial reaction zone and were large enough to allow single-crystal diffraction patterns to be obtained from them. Many of these grains have been analysed by electron diffraction and $\sim 60\%$ of them were positively identified as Ti_5Si_4 while the remainder were Ti_5Si_3. A diffraction pattern from one of these grains, which can only be indexed on the basis of Ti_5Si_4, is shown in Fig. 4a while Fig. 4b shows a lattice fringe image and

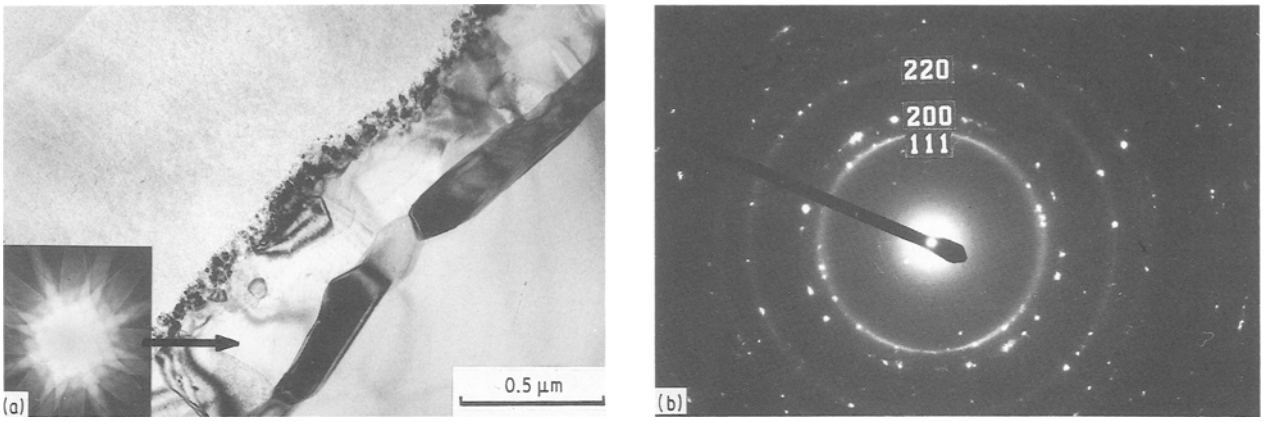

Figure 3 (a) Transmission electron micrograph of RZ of as-fabricated SCS-6/Ti–6Al–4V; two layers of the compositionally graded coating can be seen at the left. Inset: $(0\,0\,1)_{TiC}$ convergent-beam diffraction pattern from grain indicated (after slight tilt). (b) Electron diffraction pattern from the microcrystalline TiC layer of the RZ in contact with the fibre.

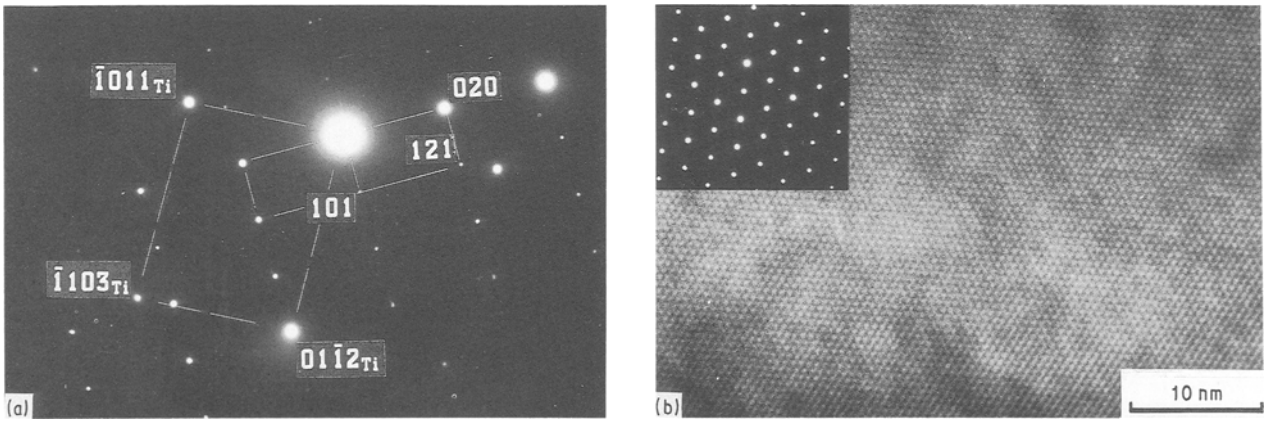

Figure 4 (a) Electron diffraction pattern of Ti_5Si_4. The matrix pattern also present is used as an internal standard. (b) Lattice fringe image and corresponding [0 0 0 1] diffraction pattern of Ti_5Si_3.

the corresponding clearly recognizable hexagonal diffraction pattern, typical of many such obtained from grains of Ti_5Si_3. EDS analyses confirmed these identifications.

While the RZ was mostly quite uniform, there were occasional areas in which it appeared almost to have penetrated the protective surface coating of the fibre, Fig. 5. Close attention was focused upon these regions, but there were no signs of chemical heterogeneity, the close presence of beta grains or other indications as to why the RZ protruded at these sites. It is, therefore, surmised that these sites represent cracks in the coating which were easily penetrated during diffusion bonding.

Upon thermal exposure the RZ became considerably thicker and more complex. After 1 h at 1000 °C the fine TiC grains at the RZ/fibre interface had coarsened appreciably, voids were clearly present in this layer, and the larger TiC single crystals had also coarsened. The composition of the outer layer of elongated grains remained unchanged, i.e. more than 50% of the grains were unquestionably Ti_5Si_4.

After more severe thermal exposure treatments, the protective layer was completely consumed and the columnar grains of the fibre began to react. The following micrographs illustrate the structure of a sample exposed for 3 h at 1050 °C in which SEM had shown the total RZ thickness to be ~ 6 μm. Fig. 6a shows the inner portion of the reaction layer. The columnar grains of the SiC fibre are seen at lower left, indicating that the compositionally graded surface layer had been completely consumed, and adjacent to them is a fine-grained layer. Analysis of electron diffraction ring patterns from this layer showed it to consist of TiC, Ti_5Si_4 and Ti_5Si_3. This is followed by a layer ~ 1.5 μm thick in which the grain size increases gradually and it is bounded, Fig. 6b, by a layer of large elongated grains of Ti_5Si_4. Convergent-beam electron diffraction patterns from individual grains in this layer again confirm the presence of the carbide and both silicides as shown by the three spectra, Fig. 6c–e from grains A, B and C of Fig. 6b. The carbides are recognizable in Fig. 6a and b from their somewhat mottled appearance. Outside the polycrystalline layers shown in Fig. 6 are alternating layers of very large TiC grains and silicides on a scale comparable with the concentric layer found by SEM. EELS analyses were conducted on many of the grains within the RZ but no evidence was obtained for the presence of a mixed Ti/Si/C phase.

Extreme difficulty was experienced in preparing satisfactory TEM samples of the entire reaction layer because of the large degree of porosity and extreme heterogeneity which led to non-uniform thinning rates. Nevertheless, the concentric layer structure first detected by SEM was also visible, Fig. 7, and analysis of individual particles within these rings confirmed the grains to be titanium carbide and the two silicides. No other phases have been confirmed in these grains and the quantities of aluminium and vanadium contained within them are less than found in the matrix. It is concluded that these elements are substitutionally combined and do not lead to the appearance of new phases.

Electron diffraction confirmed that the large angular matrix particles referred to above and shown as "Z" in Fig. 2a, were TiC particles with a pronounced dislocation substructure and apparent internal precipitation as shown in Fig. 8.

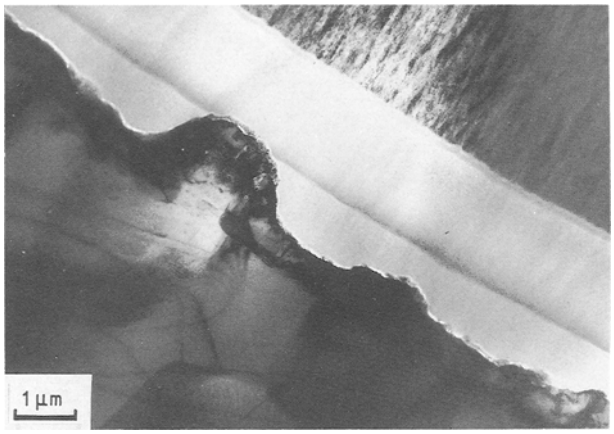

Figure 5 As-fabricated SCS-6/Ti–6Al–4V showing uneven penetration of the protective coating. (Fibre at top right.)

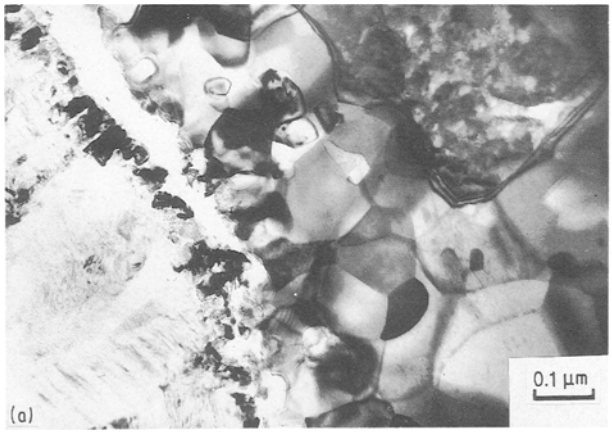

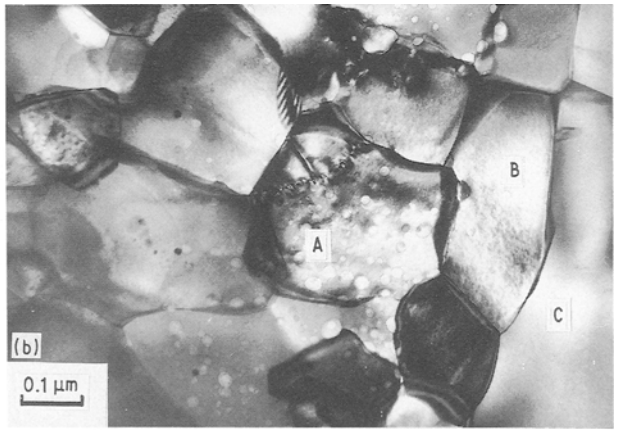

Figure 6 (a) SCS-6/Ti–6Al–4V after 3 h at 1050 °C showing columnar SiC grains of fibre at lower left; the remainder of reaction layer consists of individual grains of Ti_5Si_3, Ti_5Si_4, and TiC. (b) Extreme right-hand edge of RZ shown in (a) bounded on the right by a grain of Ti_5Si_4 (marked C). (c) EDS spectrum of crystal marked "A": analysis indicates TiC. (d) EDS spectrum of crystal marked "B": analysis indicates Ti_5Si_4. (e) EDS spectrum of crystal marked "C": analysis indicates Ti_5Si_3.

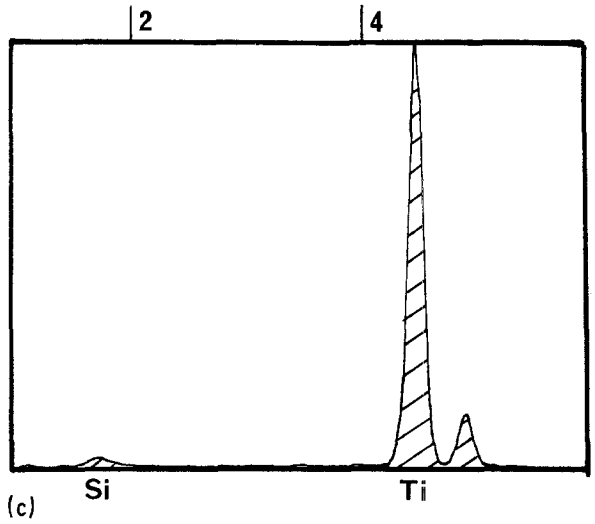

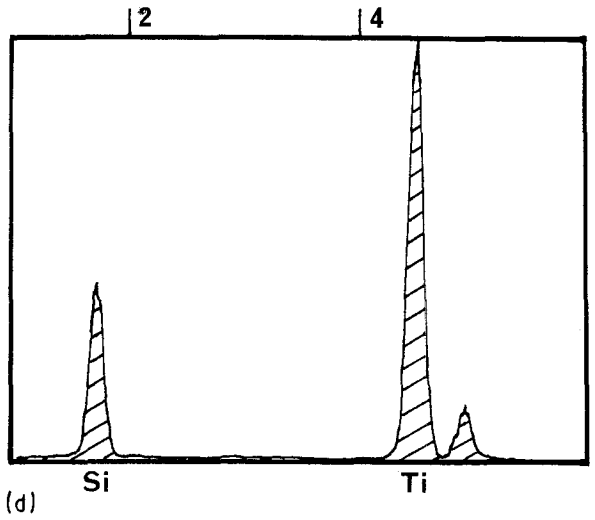

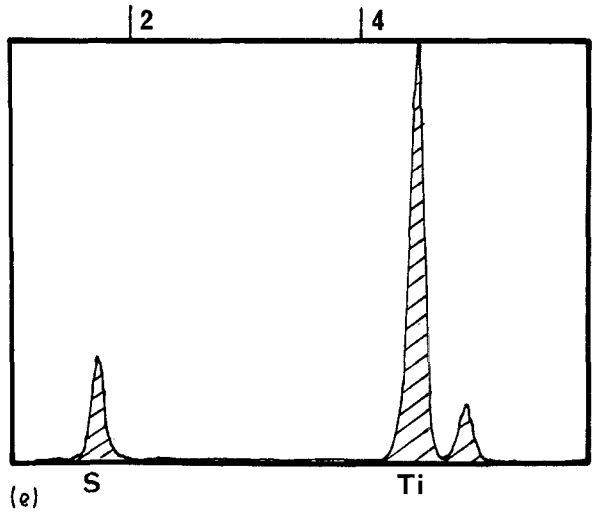

Figure 6 Continued.

As-fabricated samples of the $Ti/TiSi_2/SiC$ composite showed an extremely complex microstructure at the interface and several distinct layers were discernible, the first few of which are shown in Fig. 9a. The first layer was ~ 0.25 μm thick and consisted of small crystals as found in the SCS-6/Ti–6Al–4V composite. Immediately behind this layer, a narrow band of voids was observed. Thereafter followed a layer ~ 1.25 μm thick in which the grain size increased

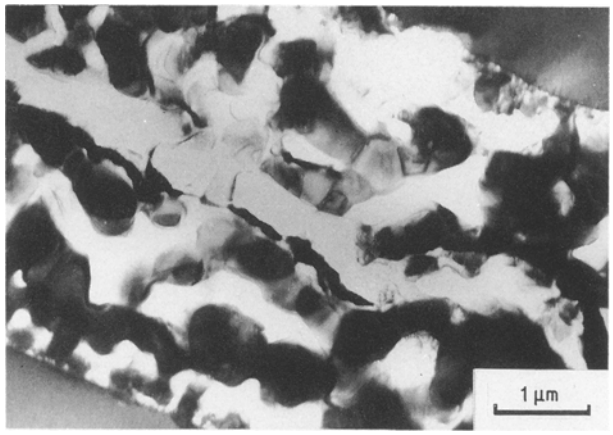

Figure 7 General view of RZ after 3 h at 1050 °C showing approximately alternating layers of reaction product.

Figure 8 TiC crystals (at left and right) in matrix of SCS-6/Ti–6Al–4V, showing mottled appearance and internal dislocations and precipitation.

steadily with distance from the fibre. Voids were observed at many locations within this layer and it was bounded by another band of voids at its outer boundary. Following this second band of voids, long grains were observed lying parallel to the fibre/matrix interface and outside this layer was a final layer, ~ 1.3 μm thick, in which the grain size was ~ 1 μm. A schematic diagram of all the layers is shown in Fig. 9b. Layer A consists of TiC and is comparable with the layer found in SCS-6/Ti–6Al–4V composites. Ring patterns from layer B could be indexed as primarily $TiSi_2$ although occasional grains of Ti_5Si_3 were also positively identified, showing that the $TiSi_2$ begins to transform to Ti_5Si_3 even during fabrication. Layer C consisted of Ti_5Si_4 and $TiSi_2$ while layer D consisted of Ti_5Si_4 and Ti_5Si_3, analogous to the outer layer in the SCS-6/Ti–6Al–4V samples. Upon isothermal exposure and consequent thickening of the reaction layer this structure coarsened considerably but no new phases were identified.

4. Discussion

The present investigation clearly indicates the complexity of the interfacial phenomena which occur in the Ti/SiC system. Considering first the SCS-6/Ti–6Al–4V system, study of the reaction kinetics

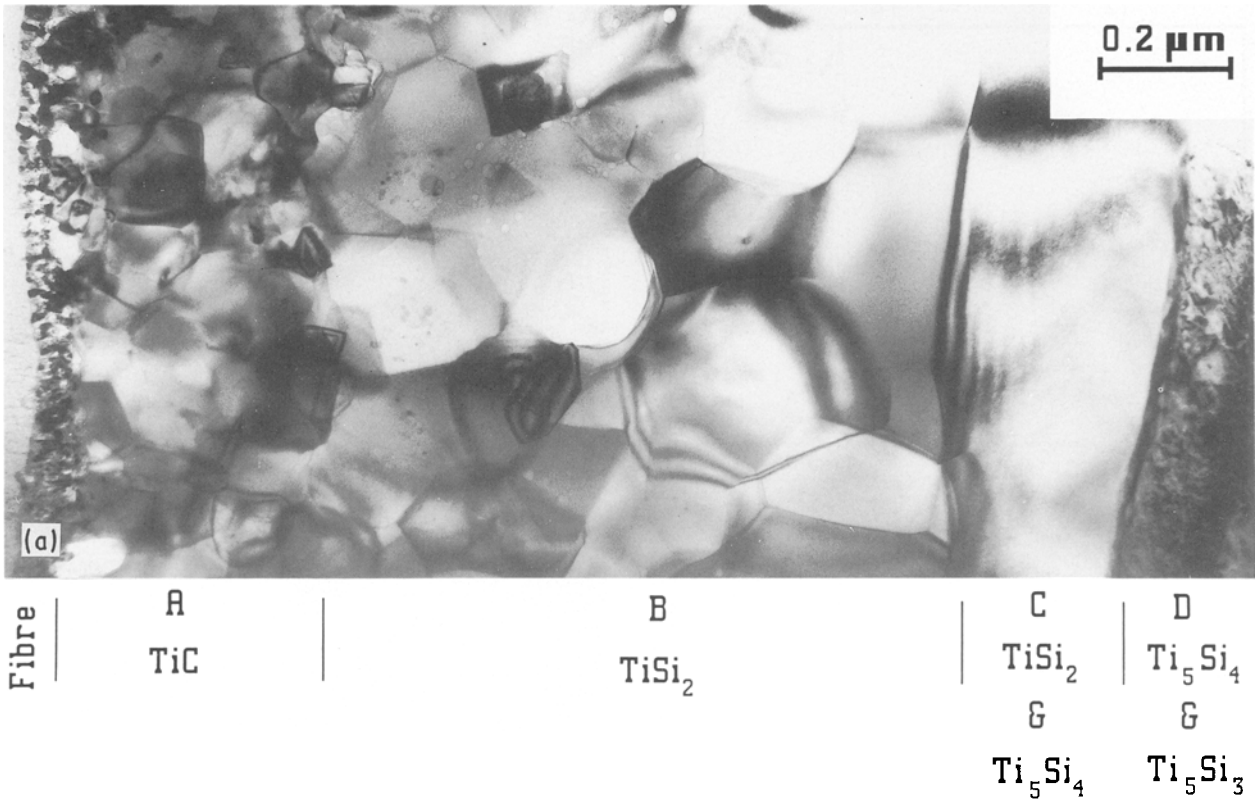

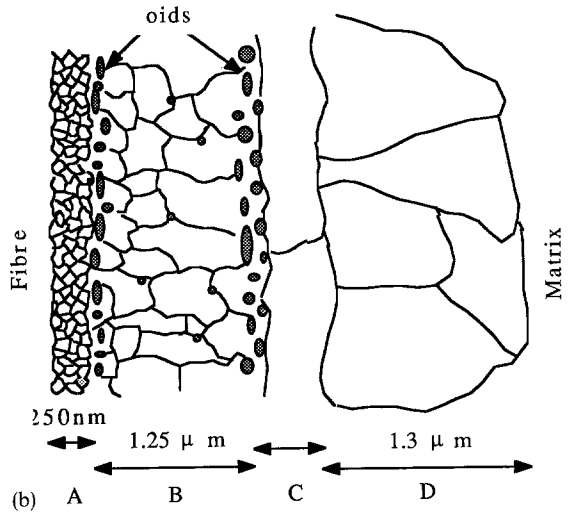

Figure 9 (a) As-fabricated $Ti/TiSi_2/SiC$ showing initial complex RZ. (b) Schematic diagram of as-fabricated $Ti/TiSi_2/SiC$ RZ illustrating principal features.

shows there to be two characteristic rate constants. The first corresponds to the early stages where the compositionally graded layer is being consumed, and the second to the later stages where the SiC fibre itself is being consumed. It is to be noted that the second is the lower rate, i.e. reaction with SiC is slower than reaction with the graded layer.

As the reaction time and/or temperature increase(s), this initial reaction layer becomes steadily thicker until the graded layer is completely consumed, after ~ 10 h at 1000 °C or ~ 2 h at 1050 °C. This characteristic reaction layer remains visible at the outside of the RZ which thereafter, thickens by formation of the concentric shells of carbide and silicide shown in Fig. 2a. Based upon the microstructural analyses it is possible to propose a mechanism for the formation of the reaction layer.

The reaction zone in the as-fabricated composite begins to form when the matrix reacts with the compositionally graded layer. TiC is the first phase to form because the outer layer consists largely, but not completely, of carbon and the Gibbs energy of TiC at 1000 °C is greater than that of any of the silicides, ~ 110 kcal mol^{-1} compared with ~ 83 kcal mol^{-1} for Ti_5Si_4 [9]. The first reaction to occur is, therefore

$$Ti + C \rightarrow TiC \quad (3)$$

followed by reactions of the type

$$9Ti + 4SiC \rightarrow 4TiC + Ti_5Si_4 \quad (4a)$$

$$8Ti + 3SiC \rightarrow 3TiC + Ti_5Si_3 \quad (4b)$$

Loo and Bastin [10] reported that carbon diffuses much more rapidly in TiC than does titanium, hence it is outward diffusion of carbon which enables further reaction. From the position of the silicides in the RZ it is also evident that silicon must also diffuse through the TiC. It should be noted that two silicides and a carbide form, indicating the existence of a three-phase region in the Ti–Si–C ternary phase diagram.

Once the carbon-rich layer has been consumed, reactions, 4a and b begin to occur but the free energy changes for these reaction are lower and the reactants must first diffuse through an RZ of appreciable thickness. For these reasons the reaction rate decreases as the alternating layers of carbide and silicide are formed. SEM, EDS and electron diffraction showed that these phases occurred in almost concentric shells, the number of shells increasing with exposure time. In

addition to the phases present, the other significant microstructural feature is the presence of a large number of voids. While some of these are dispersed throughout the structure, they are significantly concentrated in bands within certain regions of the concentric shell structure, see for example, Figs 6 and 9.

It is postulated, then, that the reaction layer develops at first by the formation of a stratified structure of carbide and silicides which form a significant diffusion barrier to further thickening. As it grows, therefore, the layer at first offers increasing protection, the common parabolic rate behaviour. As it develops, however, it is accompanied by the formation of a large number of voids which ultimately connect and/or provide short-circuit diffusion paths through the semi-protective layer. Also, cracking of the RZ occurs due to local volume changes, creating further rapid diffusion paths.

Consequently, at some stage, the layer becomes porous and essentially non-protective, allowing rapid reaction to proceed again. This reaction evidently proceeds at the reaction zone/fibre interface, indicating that rapid diffusion of titanium through the layer is now occurring. The sequence of building up a protective layer, followed by its breakdown and subsequent rapid reaction is repeated at intervals and each time leads to another set of concentric rings. The measured apparent activation energy for the process is $\sim 74\ \text{kcal mol}^{-1}$ and is close to the value of 79 kcal mol^{-1} reported for the activation energy for diffusion of carbon in TiC [10]. It is probable, therefore, that it is primarily the TiC which is responsible for reducing the reaction rate.

The original observation of titanium silicides in the reaction layer indicated that deliberate deposition of a silicide may decelerate the reaction. Hence, experiments were conducted with a deposited layer of $TiSi_2$ on the surface of an SiC fibre. However, even in this composite, the structure of the RZ ultimately tended towards that of the SCS-6/Ti–6Al–4V composite. That is, a fibre/RZ layer of fine carbides was followed by approximately stratified layers of carbide and silicide. Again, it was found that two silicides were formed and that the RZ contained a significant volume fraction of voids.

The observations have shown that extensive and complex fibre/matrix reactions occur but they yield a common conclusion as to what the final, thermodynamically stable interfacial microstructure will be under the present conditions of temperature and environment. The structures in each case tend towards a mixture of TiC, Ti_5Si_3 and Ti_5Si_4 and deposition of one of these phases will not totally prevent further reaction, especially if it cannot be deposited and maintained defect-free. The reaction products were, in each case, the same, even though the matrices were different and an initial $TiSi_2$ layer was present in one case. Clearly $TiSi_2$ is unstable under these conditions and will transform to the other two silicides.

The large volume fraction of voids appears to be extremely deleterious, because it leads to breakdown of the protective layer. While it is generally well-known that voids are undesirable because they can act as stress raisers, the present observations also show that they must be eliminated from the RZ in order to reduce the reaction rate. In the SCS-6/Ti–6Al–4V system the voids arise principally through the Kirkendall effect, whereas in the $Ti/TiSi_2/SiC$ system they arise also due to pores present in the chemical vapour deposited $TiSi_2$ layer. Thus, although it may be possible to tailor surface coatings to reduce this effect, particular attention must be paid to the manner in which the coating is applied so as to reduce the porosity as far as possible.

At least three phases have been definitely identified by electron diffraction and EDS analyses in the RZ of these SiC/Ti systems, including the Ti_5Si_4 phase which was not identified in previous investigations. In agreement with the results of Choi *et al.* [11], the phase in contact with SiC was found to be TiC while those in contact with the titanium were silicides. However, no amorphous region was found and no evidence was found for the existence of the Ti_3SiC_2 phase which has been found by previous authors [8, 11]. This may be due to its low volume fraction as reported by Choi *et al.* or it may be that this is a metastable phase which occurs at shorter times and/or lower temperatures than those used here. Heikinheimo *et al.* [12] found that, in binary Si/Ti couples annealed at 1100 °C, all possible silicides formed starting with $TiSi_2$ and TiSi at short times followed at longer times by Ti_5Si_4, and finally Ti_3Si and Ti_5Si_3 at times > 10 h. However, in spite of the stratified appearance of the RZ, only two of these silicides were found in the present work.

Earlier studies of the ternary Ti–Si–C system by Brukl [13] have frequently been used as a point of reference in previous studies but it would appear that their section at 1200 °C is not an accurate representation of the situation at lower temperatures. It seems highly desirable to the present authors that this potentially important system should be re-evaluated.

The Ti_3AlC phase is not a component of the RZ itself. It apparently forms as aluminium is rejected from the matrix and its concentration builds up ahead of the advancing interface. Little is known about this phase but it may warrant further examination as a candidate for coating.

The mottled appearance of the TiC grains is in agreement with the work of Konitzer and Loretto [14, 15] who studied Ti–6Al–4V/TiC composites and found non-stoichiometric titanium carbide in contact with the matrix after heat treatment at temperatures between 950 and 1050 °C. This non-stoichiometry may be intimately linked to the mechanism by which the semi-protective layer breaks down.

Further work, preferably at first on model materials is necessary to generate the composition and diffusion data base required for further progress in this sytem. Finally, because the reaction zones investigated here have been extremely thick, it is worth emphasizing that most studies to date, including this one, indicate that the reaction rates at $T < 800$ °C are very low. Thus, interfacial reaction in service at the maximum anticipated use temperatures of titanium metal matrix composites does not present a significant threat to their safe use.

5. Conclusions

1. The reaction products formed between titanium and the SiC fibres studied here are TiC, Ti_5Si_4, Ti_5Si_3.

2. Ti_3AlC forms in the later stages of isothermal exposure of SCS-6/Ti–6Al–4V.

3. The reaction rate decreases once the carbon-rich layer of the SCS-6 fibre has been consumed.

4. TiC offers promise as a protective layer, possibly doped to reduce its defect structure.

5. Extensive porosity develops in the reaction zone. It is desirable to eliminate all sources of porosity in the RZ.

Acknowledgement

One of the authors (I.W.H.) gratefully acknowledges financial support from the Centre Nationale de la Recherche Scientifique, and the provision of research facilities by Professor J. Etourneau, Département de Chimie du Solide du CNRS, University of Bordeaux, during the performance of some of this work.

References

1. R. KIESCHKE, R. SOMEKH and T. W. CLYNE, "Proceedings of the 3rd European Conference on Composite Materials" edited by A. R. Bunsell, P. Lamicq and A. Massiah, Bordeaux 1989 (Elsevier, London, 1989) p. 265
2. C. G. RHODES and R. A. SPURLING, ASTM STP 864 (ASTM, Philadelphia, PA, 1985) p. 585.
3. H. J. DUDEK, L. A. LARSON and R. BROWNING, *Surf. Interface Anal.* **6** (1984) 274.
4. W. J. WHATLEY and F. E. WAWNER, *J. Mater. Sci. Lett.* **4** (1985) 173
5. D. B. GUNDEL and F. E. WAWNER, in "14th Annual Conference on Composite Materials and Advanced Structures", January 1990, Cocoa Beach, FL.
6. B. A. LERCH and D. R. HULL, NASA Tech. Mem., TM-100938, 1988.
7. I. W. HALL, J.-L. LIRN and J. RIZZA, *J. Mater. Sci. Lett.*, **10** (1991) 236.
8. P. MARTINEAU, R. PAILLER, M. LAHAYE and R. NASLAIN, *J. Mater. Sci.* **19** (1984) 2749.
9. J. L. MURRAY (ed.), "Binary Phase Diagrams of Ti Alloys" (ASM International, Metals Park, OH, 1987).
10. F. J. J. LOO and G. F. BASTIN, *Metall. Trans.* **20A** (1989) 403.
11. S. K. CHOI, M. CHANDRASEKARAN and M. J. BRABERS, *J. Mater. Sci.* **25** (1990) 1957.
12. E. HEIKINHEIMO, J. KIVILAHTI and M. PAJUNEN, in "Microbeam Analysis", edited by D. E. Newbury (San Francisco Press, CA, 1988) p. 509
13. C. E. BRUKL, in "Ternary Phase Equilibria in Transition Metal-Boron-Carbon-Silicon Systems", Part II, Vol. VII, AFML-TR-65-2 (US Department of Commerce, Springfield, VA, 1965) p. 425.
14. D. G. KONITZER and M. H. LORETTO, *Acta. Metall.* **37** (1989) 397.
15. *Idem., Mater. Sci. Engng* **A107** (1989) 217.

Received 22 March
and accepted 1 July 1991